Characterization of Oligomers during α-Synuclein Aggregation Using Intrinsic Tryptophan Fluorescence[†]

Alexandra Dusa, Joanna Kaylor, Shauna Edridge, Nika Bodner, Dong-Pyo Hong, and Anthony L. Fink*

Department of Chemistry and Biochemistry, University of California, Santa Cruz, California 95064

Received July 20, 2005; Revised Manuscript Received October 2, 2005

ABSTRACT: The aggregation of the presynaptic protein α-synuclein is associated with Parkinson's disease (PD). The details of the mechanism of aggregation, as well as the cytotoxic species, are currently not well understood. α-Synuclein has four tyrosine and no tryptophan residues. We introduced a tyrosine to tryptophan mutation at position 39 to create an intrinsic fluorescence probe and allow additional characterization of the aggregation process. Y39W α-synuclein had similar fibrillation kinetics (2-fold slower), pH-induced conformational changes, and fibril morphology to wild-type α-synuclein. In addition to intrinsic Trp fluorescence, acrylamide quenching, fluorescence anisotropy, ANS binding, dynamic light scattering, and FTIR were employed to monitor the kinetics of aggregation. These biophysical probes revealed the significant population of two classes of oligomeric intermediates, one formed during the lag period of fibrillation and the other present at the completion of fibrillation. As expected for a natively unfolded protein, Trp 39 was highly solvent-exposed in the monomer and is solvent-exposed in the two oligomeric intermediates; however, it is partially, but not fully, buried in the fibrils. These observations demonstrate the utility of Trp fluorescence labeled α-synuclein and demonstrate the existence of an oligomeric intermediate that exists as a transient reservoir of α-synuclein for fibrillation.

Parkinson's disease (PD)[1] is the second most common neurodegenerative disease, affecting 1−2% of the population over age 65. It involves loss of dopaminergic neurons in the *substantia nigra*, which leads to decreased dopamine levels in the striatum, causing symptoms such as tremors, rigidity in muscles, and bradykinesia (*1*−*3*). While the exact cause of PD is not known, aggregation of the presynaptic protein α-synuclein is believed to play a critical role in the etiology of the disease (*4*−*15*).

Wild-type α-synuclein is a 140 amino acid protein, showing little or no ordered structure under physiological conditions in vitro (*16*). The overall structure of α-synuclein includes a highly conserved N-terminal domain (residues 1−95) containing seven 11 amino acid repeats with a consensus sequence, KTKEGV, a lipid binding motif. The acidic C-terminal domain contains three of the four tyrosine residues, at positions 125, 133, and 139. The fourth Tyr residue is at position 39. These Tyr residues are conserved in all of the α-synuclein orthologues (*17*, *18*).

The Y39W α-synuclein was created for the purpose of monitoring potential structural changes during the aggregation process. Such an intrinsic fluorescent probe is less likely to have significant effects on the properties of α-synuclein and its aggregation than more bulky side-chain-modified fluorescence labels. The presence of a single tryptophan residue facilitates interpretation of the environment around position 39 during aggregation, since the fluorescence emission of Trp undergoes a blue shift when the polarity of its environment decreases. Recently, a number of Trp-nitroTyr α-synucleins were prepared and examined for FRET (nitroTyr quenches Trp fluorescence), including Trp 39-nitroTyr 19 and Trp 4-nitroTyr 19 (*19*). Monomeric α-synuclein was examined both in aqueous solution and when bound to SDS micelles and revealed the presence of compact, intermediate, and extended conformations.

The results of the present investigation indicate that the intrinsic fluorescence of Trp 39 is a useful probe for the α-synuclein aggregation process, revealing the presence of two oligomeric intermediates, one formed during the lag period of fibrillation and the other present at completion of the fibrillation. In addition, the data demonstrate that residue 39 becomes partially buried in the fibrils but is solvent-exposed in the monomer and in the transient oligomers formed during fibrillation.

MATERIALS AND METHODS

Materials. Thioflavin T (ThT) and 1-anilinonaphthalene-8-sulfonic acid (ANS) were obtained from Sigma, St. Louis, MO. All other chemicals were of analytical grade from Fisher Chemicals.

Expression of WT and Y39W α-Synuclein. The mutant was created through site-directed mutagenesis, using the QuickChange site-directed mutagenesis kit from Stratagene. The primers, from IDT Inc., were diluted to a final concentration of 126 ng/μL, and a 1 μL aliquot of the dsDNA plasmid template (25 ng/μL) was used. Before transformation into the expression cell line, the plasmids were sequenced to validate the presence of the desired mutation. Mass spectrometry and/or western blots were also performed on the

[†] This research was supported by Grant NS39985 from the National Institutes of Health.

* To whom correspondence should be addressed. Phone: (831) 459-2744. Fax: (831) 459-2935. E-mail: enzyme@cats.ucsc.edu.

[1] Abbreviations: PD, Parkinson's disease; ThT, thioflavin T; CD, circular dichroism; SEC, size-exclusion chromatography; ATR, attenuated total reflectance.

10.1021/bi051426z CCC: $33.50
Published on Web 02/07/2006

expressed proteins to confirm the molecular weight changes expected from the mutations. On the basis of SDS−PAGE, which showed a single band, both wild-type and Y39W α-synucleins were >95% homogeneous.

Purification of the α-Synucleins. Wild-type (or mutant) α-synuclein plasmid (pRK172), containing a carbenicillin resistance gene and the T7 promoter gene, was transfected into *Escherichia coli* BL21(DE3) cells. Cells were harvested, lysed, precipitated with ammonium sulfate between 30% and 50% saturation, and collected at 4000 rpm and 4 °C for 15 min. The 50% ammonium sulfate precipitate was dialyzed overnight and run on a DEAE-Sepharose fast-flow column at 4 °C. A 50−500 mM NaCl gradient was established and ∼70−80 6 mL fractions were collected. The fractions determined to have high α-synuclein content by SDS−PAGE were pooled together and dialyzed against deionized water at 4 °C. The concentration was determined by A_{276}, and aliquots containing 10 mg of protein were lyophilized and stored at −80 °C. Extinction coefficients used were $\epsilon_{276nm} = 0.401$ and 0.673 $(mg/mL)^{-1}$ for wild-type and Y39W α-synuclein, respectively.

Mass Spectrometry. A MicroMass Quattro II electrospray mass spectrometer was used to obtain mass spectra. Samples were made by preparing a 2 mL solution of 10 μM protein in a 50% acetonitrile/H_2O mixture. Samples were adjusted to pH 2.0 with 12 M HCl immediately before use. Injection was carried out using a syringe pump (Harvard Apparatus, Holliston, MA) at a flow rate of 6 μL/min. The source temperature was set to 90 °C, the capillary voltage was 3.0 kV, and electrospray positive ionization mode was used.

Aggregation of α-Synuclein. The kinetics of fibril formation were monitored with ThT fluorescence assays on sample mixtures containing 2 mg/mL α-synuclein, 150 mM NaCl, 20 mM phosphate buffer, and 20 μM ThT. Plate reader measurements were carried out in 96-well plates at 37 °C, with 120 rpm shaking with a 20 mm shaking diameter, and 3 mm glass beads. Manual ThT fluorescence measurements, performed on a Fluoromax-3 (Jobin-Yvon Horiba) spectrofluorometer, were monitored at 37 °C in glass vials, stirred with micro-stir bars, using the same protein and salt concentrations as above. Aliquots (10 μL) of the protein mixture were removed at various time points and added to a cuvette containing a 1 mL solution of 20 μM ThT and 20 mM buffer. The solution was excited at 450 nm, and emission was scanned between 470 and 560 nm. The intensity at 482 nm was recorded and plotted against time. Each experiment was repeated at least three times, to verify reproducibility; errors were of the order of ±10−15%. The ThT fluorescence curves were fitted with a sigmoidal curve as previously described (*20*).

Preparation of Pellet and Supernatant Samples. Aliquots of 140 μL were removed from the incubation solutions at various time points and centrifuged for 45 min at 14K. The supernatant was removed and analyzed separately, and the pellet was washed twice, resuspended in 140 μL of the same buffer used to prepare the samples (100 mM NaCl, 20 mM phosphate, pH 7.4), and subsequently analyzed.

Intrinsic Fluorescence. Aliquots (20 μL) of the Y39W α-synuclein incubation mixture were removed at various time points and mixed into a cuvette containing a 1 mL solution of 150 mM NaCl and 20 mM phosphate, pH 7.4. To minimize fluorescence contribution from the tyrosine residues, the samples were excited at 290 nm and emission was scanned between 300 and 440 nm. Spectra were plotted, and the wavelength and intensity at the maximum emission were recorded. Dityrosine fluorescence was measured with excitation at 310 nm.

Acrylamide Quenching. Aliquots of the same protein incubation solutions were drawn at various time points during the course of fibrillation and mixed with increasing concentrations of acrylamide, from 0.1 to 0.6 M. This was performed on both the solution mixture and the supernatant alone. The intrinsic fluorescence was recorded before and after addition of the quencher. The Stern−Volmer equation describes collisional quenching processes:

$$I_0/I = 1 + K_{sv}[Q]$$

where I_0 is the fluorescence intensity prior to the addition of the quencher, I is the intensity after quencher addition, and [Q] is the concentration of acrylamide in this case. High K_{sv} values indicate a high degree of quenching and therefore high Trp accessibility. Stern−Volmer plots for the Y39W supernatant were fitted with the equation $F_0/F = (1 + K_{sv}[A]) \exp(K_{st})[A])$, where F_0 and F are the intrinsic fluorescence intensities in the absence and presence of acrylamide, respectively, [A] is the concentration of the acrylamide, K_{sv} is the Stern−Volmer constant for dynamic quenching, and K_{st} is the static component of the quenching process (*21*).

Fluorescence Anisotropy. Samples of the protein incubation mixture and supernatant were excited with vertically polarized light, and the emission intensity was measured through both parallel and perpendicular polarizers ($I_{||}$ and $I_{\perp}$). The anisotropy, r, a dimensionless quantity, is defined as

$$r = (I_{||} - I_{\perp})/(I_{||} + 2I_{\perp})$$

By comparing anisotropy values as a function of time, it is possible to measure changes in the relative mobility of the fluorophore throughout the aggregation process. Excitation was at 290 nm and emission at 350 nm.

ANS Fluorescence. 1-Anilinonaphthalene-8-sulfonic acid (ANS) is a dye whose fluorescence is greatly enhanced on binding to hydrophobic surfaces, displaying a characteristic blue shift in its fluorescence maximum from ∼515 to ∼475 nm. Partially folded intermediate species are characterized by exposure of hydrophobic patches, and their presence can thus be monitored by changes in the fluorescence emission of ANS over time. Aliquots (20 μL) of the incubation mixture were removed at various time points and mixed into a cuvette containing a 1 mL solution of 5 μM ANS and 20 mM phosphate buffer, pH 7.4. Initial experiments were performed to identify the optimum ANS concentration. Samples were excited at 350 nm, and emission was scanned between 360 and 600 nm. The wavelength of maximum emission was recorded and plotted against time. Intensities at λ_{max} were also noted.

Circular Dichroism. Far-UV CD measurements were performed with an AVIV 60DS spectrophotometer, with a 0.01 cm path length cuvette. Solutions were 1 mg/mL protein, 100 mM NaCl, and 20 mM buffer. Spectra were recorded from 250 to 190 nm with a step size of 0.5 nm, a bandwidth of 1.5 nm, and an averaging time of 4 s. An average of three

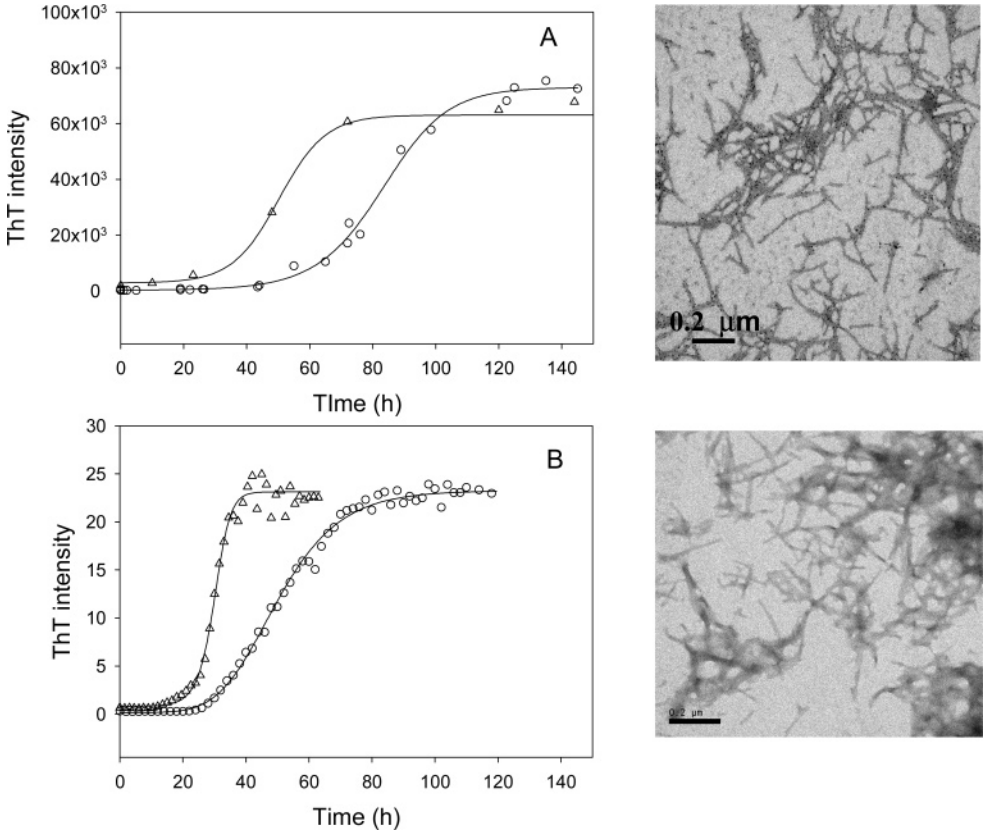

FIGURE 1: Kinetics of fibril formation by Y39W and wild-type α-synuclein monitored by ThT fluorescence. (A) Manual assays (2 mg/mL protein). (B) Plate reader assays (1 mg/mL protein). Key: Y39W (△) and WT (○). Conditions: pH 7.4, 150 mM NaCl, and 20 mM PBS. The images on the right are from TEM and show the wild-type fibrils in the top image and the Y39W fibrils in the bottom image. The scale bars are 200 nm.

to five scans was obtained for each spectrum. Separate buffer spectra were also collected and subtracted from the protein spectra.

Fourier Transform Infrared Spectroscopy. ATR-FTIR data was collected on a ThermoNicolet 670 spectrometer equipped with an MCT detector. The samples were spread out and dried as a thin film on a germanium IRE, with a constant flow of nitrogen gas. Between 256 and 1024 interferograms were collected for each sample. Samples were 2 mg/mL protein, 150 mM NaCl, and 20 mM phosphate buffer. Data analysis was performed with the GRAMS32 software from Galactic Industries. Secondary structure components and percentages were estimated by curve fitting following Fourier self-deconvolution and second derivatives (*22*).

Monitoring α-Synuclein Association by Dynamic Light Scattering. DLS measurements were performed at 20 °C using a DynaPro (Wyatt Technology) model 99-E-50 instrument. Aliquots of 10 μL of the incubation solution were centrifuged before measuring DLS. One microliter of the supernatant was diluted with 10 μL of filtered buffer in the DLS cuvette, and measurements were taken within 3−7 min. Scattering peaks less than 0.1 nm radius and more than 1000 nm were ignored.

Electron Microscopy. Transmission electron microscopy was used to visualize the fibrils and/or amorphous aggregates present at the end of the aggregation process. Samples (5 μL) were placed onto carbon-coated grids, washed with deionized water, and negatively stained with 1% uranyl acetate. They were viewed with a JEOL electron microscope, and the images were recorded at a 75K magnification.

RESULTS

Comparison of Y39W and Wild-Type α-Synuclein. (A) Fibrillation of Y39W α-Synuclein Is Similar to That of Wild-Type α-Synuclein. Protein aggregation and fibrillation kinetics typically appear sigmoidal, usually attributed to a nucleated polymerization process in which the initial lag phase corresponds to formation of a critical nucleus, the subsequent exponential growth phase corresponds to fibril elongation, and the final leveling off is ascribed to exhaustion of soluble monomers and intermediates. The kinetics of fibrillation for both wild-type and Y39W α-synuclein were monitored using ThT fluorescence. The data (Figure 1) indicate that Y39W α-synuclein forms fibrils somewhat more slowly than wild type and that both the nucleation phase and fibril elongation were slower with the mutant. In addition, the data in Figure 1 show that the rate of fibrillation was slower in the manual assays (which had twice the protein concentration) compared to the plate reader: Y39W α-synuclein displayed an average lag time of 26 ± 4 h on the plate reader and 50 ± 7 h for the manual assays, reflecting the different amounts of agitation in the two types of assays. Examination of the morphology of the fibrils by negative staining electron microscopy indicated that fibrils from both wild-type and Y39W α-synuclein appeared indistinguishable (Figure 1).

(B) Y39W and Wild-Type α-Synuclein Have Similar Conformations. The secondary structure of Y39W α-synuclein was examined at pH 7.4 and 3.2 and compared to wild type. At pH 7.4 the far-UV CD spectra of both proteins

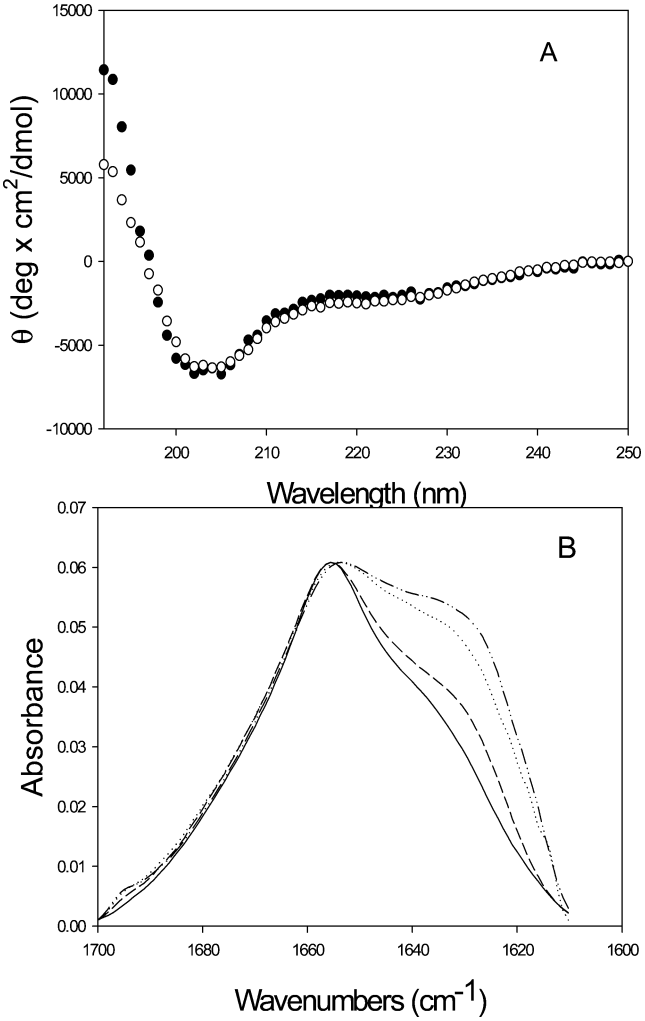

FIGURE 2: Comparison of secondary structure of WT and Y39W α-synuclein. (A) Far-UV CD spectra of Y39W (open circles) and WT (closed circles) at pH 7.4 showing that both proteins are largely unstructured. (B) FTIR spectra of Y39W (pH 7.4, dotted line; pH 3.2, dash−dot line) and WT (pH 7.4, solid line; pH 3.2, dashed line). An increase in secondary structure, specifically β-sheet at ~1630 cm^{-1}, is observed as the pH is decreased.

had the characteristics of an unfolded protein (Figure 2A). The spectra for WT and Y39W were essentially superimposable, indicating a similar overall structure at pH 7.4. Similarly, at the lower pH, both Y39W and WT had essentially identical far-UV CD spectra (data not shown), corresponding to a partially folded conformation (*23*).

The secondary structure was also investigated with FTIR, which is more sensitive to β-structure than CD. Spectra for Y39W and WT were obtained at pH 7.4 and 3.2 and showed an enlarged shoulder in the vicinity of 1630 cm^{-1}, corresponding to increased β-structure for the Trp mutant at both pHs (Figure 2B). We have previously shown that wild-type α-synuclein forms an amyloidogenic partially folded intermediate at pH 3, accounting for the difference in spectra between pH 7 and 3 (*23*). The secondary structure content of both proteins at each pH was estimated after curve fitting following deconvolution with Fourier self-deconvolution and second derivatives. The analysis for Y39W showed a larger fraction of β-sheet/extended structure at pH 7.4 (27 ± 6%), compared to WT (19 ± 6%), suggesting somewhat more structure in the natively unfolded monomer in the presence

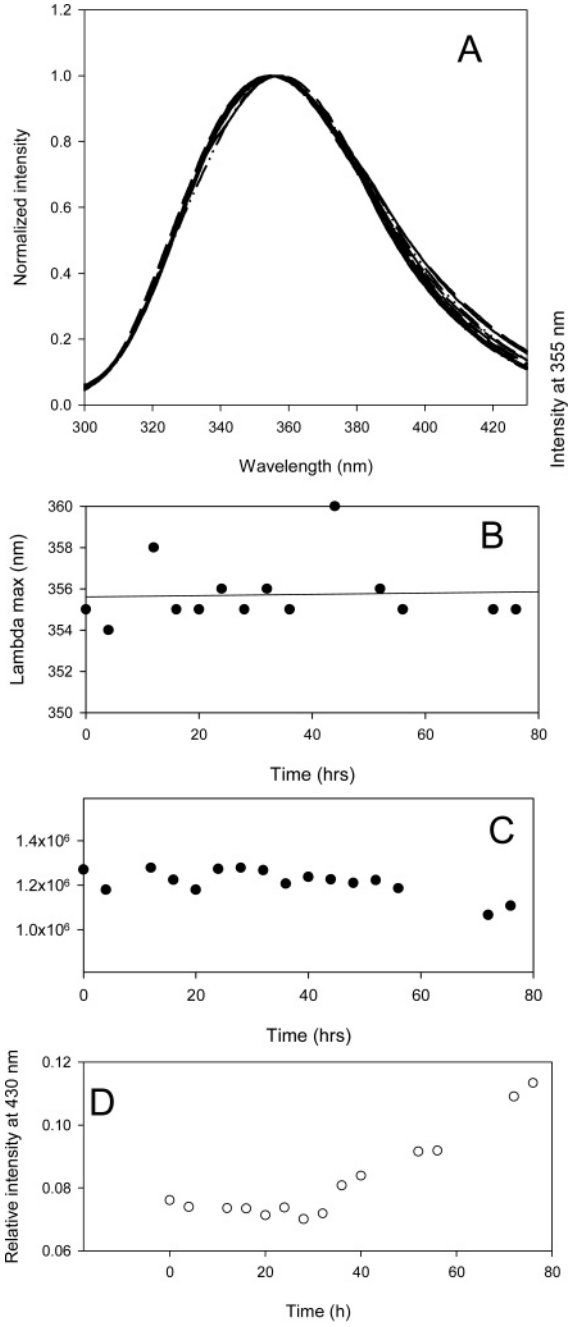

FIGURE 3: Changes in the intrinsic Trp fluorescence of the supernatant during incubation of Y39W α-synuclein at 37 °C. (A) λ_{max}-normalized emission spectra of the supernatant as a function of wavelength monitored over time. (B) Plot of λ_{max} vs time for the intrinsic fluorescence of the Y39W supernatant, indicating no changes in the environment of Trp 39 with time. (C) Plot of the maximum intensity vs time for the intrinsic fluorescence of the Y39W supernatant, indicating no changes in the environment of Trp 39 with time. (D) Change in fluorescence emission intensity at 430 nm on excitation at 300 nm changes in emission intensity relative to the initial spectrum, attributed to the formation of dityrosine. Unless otherwise noted all incubations were at 37 °C, pH 7.4, and 150 mM NaCl.

of the mutation. The value of 19 ± 6% found here is in agreement with other reports.

Monitoring Time-Dependent Structural Changes during Incubation of α-Synuclein. α-Synuclein aggregation and fibrillation was accomplished by incubating 140 μM wild-type or Y39W α-synuclein in 20 mM phosphate buffer, pH 7.4, containing 150 mM NaCl. Under these experimental

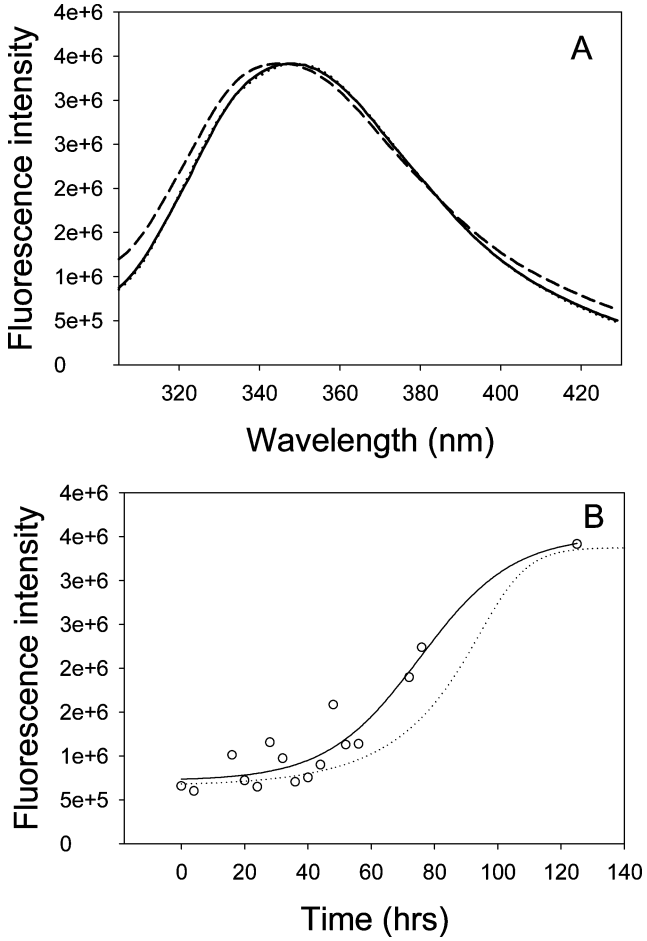

FIGURE 4: Changes in the intrinsic Trp fluorescence of the pellet during incubation of Y39W α-synuclein at 37 °C. (A) Pellet intrinsic fluorescence at 48 h (solid line) and 125 h (dashed line). (B) Increase in Trp fluorescence intensity at 346 nm as a function of time of incubation (○). The dotted line is the increase in ThT fluorescence, reflecting fibril formation.

conditions with mild agitation (stirring) the lag time was ~50 h (run-to-run variations were ±15%). Aliquots were withdrawn for analysis at various time periods over a 6 day period. The samples were separated by centrifugation into soluble (supernatant) and insoluble (pellet) fractions. In the first 60−70 h the majority of the protein is in the supernatant; at later times the majority is in the pellet.

(A) Intrinsic Fluorescence of the Supernatant and Pellet during Incubation of Y39W. During incubation, the wavelength of maximum fluorescence emission was monitored in order to detect changes in the environment and solvent accessibility of the Trp. The emission λ_{max} of the supernatant (excitation at 290 nm) remained effectively constant over 70 h at values between 354 and 356 nm, which is indicative of substantial solvent exposure of the Trp (Figure 3A,B). A plot of the intensity at 355 nm against time of incubation also indicates no significant changes in the environment of Trp 39 (Figure 3C). Interestingly, at later times in the lag phase, and during the exponential growth phase, an increase in intensity at high wavelengths was observed (Figure 3A,D). This could reflect formation of a small amount of dityrosine, whose excitation λ_{max} is around 310 nm (see below).

A pellet following centrifugation was only visible after the 48 h time point, which is consistent with the ThT fluorescence results showing a lag time of 50 h. The Trp

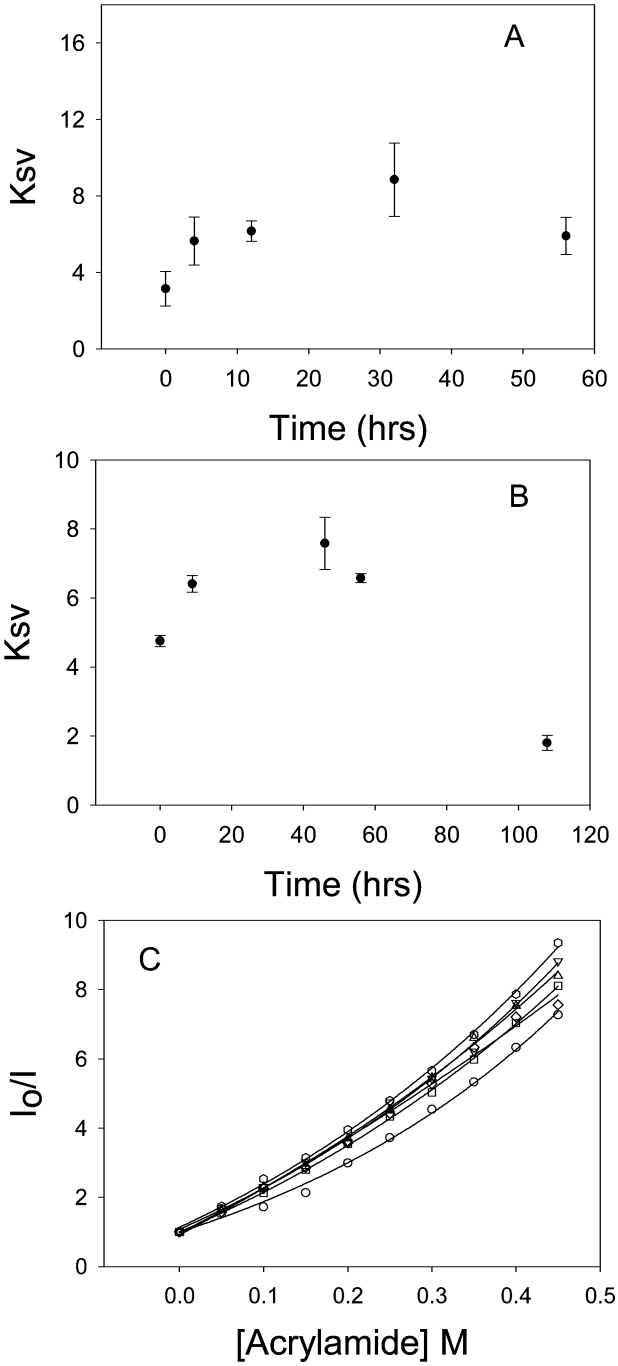

FIGURE 5: Solvent accessibility of Trp 39 measured by acrylamide quenching of Trp fluorescence as a function of time of incubation. (A) Stern−Volmer constant as a function of incubation time for the supernatant. An increase in K_{sv} indicates increased solvent exposure of the Trp. (B) Stern−Volmer constant as a function of incubation time for the total incubation mixture, showing the decreased accessibility of Trp 39 in the fibrils. Note the different time scales in panels A and B. (C) Stern−Volmer plot for the supernatant over time (0 h, open circles; 4 h, inverted triangles; 12 h, squares; 20 h, diamonds; 32 h, triangles; 56 h, hexagons).

fluorescence of the resuspended pellet showed a significant blue shift compared to the monomer (Figure 4A), with an emission λ_{max} of 346 ± 2 nm. In addition, a time-dependent increase in the emission intensity at the λ_{max} was also observed (Figure 4B), which closely paralleled the rate of fibril elongation, based on the ThT trace, and reflects the increasing amount of fibrils with increased incubation time. The shift in λ_{max} to 346 nm points to Trp 39 becoming

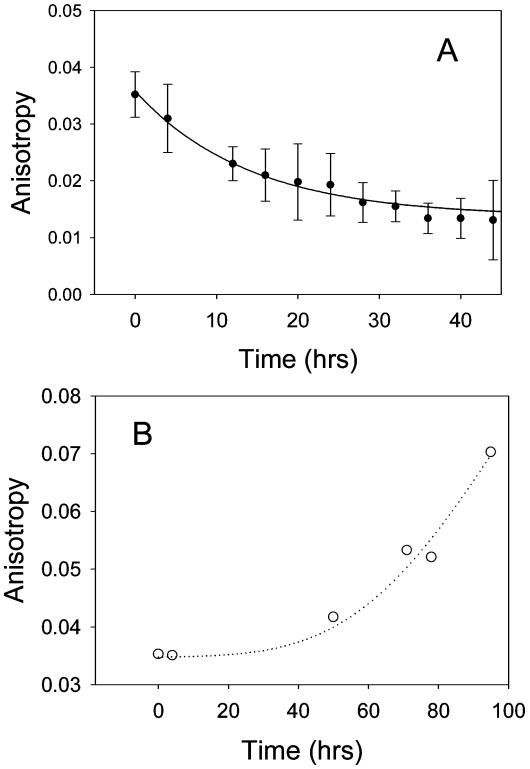

FIGURE 6: Changes in the fluorescence anisotropy during the incubation of Y39W α-synuclein. (A) Data for the supernatant; the decrease in anisotropy was fit to a single exponential. (B) Data for the mixture.

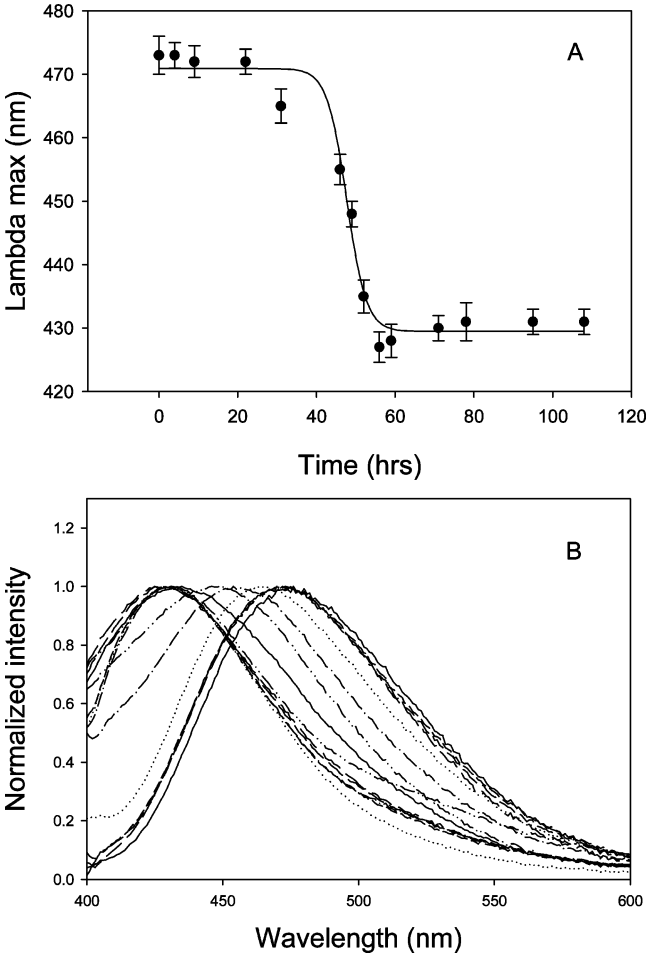

FIGURE 7: Changes in ANS binding during incubation of Y39W α-synuclein. (A) Plot of λ_{max} vs time for ANS fluorescence, for the mixture, fits a sigmoidal curve and shows no significant blue shifts over the period corresponding to the lag time. (B) λ_{max}-normalized ANS fluorescence emission spectra for the incubation mixture monitored over time. The first 36 h displays almost superimposable spectra. Blue shifts start occurring during the period corresponding to fibril formation and growth (>40 h). The time scale covered by the spectra is 0−108 h, with the blue shift increasing with time.

significantly more buried in the fibrils. There was a small, progressive blue shift in the λ_{max} of the pellet with increasing time, suggesting the possibility of small changes in fibril morphology as time progressed, probably reflecting association between fibrils, e.g., clumping, as observed in EM images.

(B) Acrylamide Quenching To Measure Trp Solvent Accessibility. When aliquots of the Y39W *supernatant* were removed at various time points during the incubation and mixed with acrylamide to measure solvent exposure of Trp 39, a time-dependent increase in the Stern−Volmer constant (K_{sv}) was observed, reaching a maximum at the end of the lag phase (Figure 5A). This corresponds to the Trp becoming more exposed as aggregation proceeds during the lag time. If we assume that the supernatant is composed of monomers and soluble oligomers (see below), this change in K_{sv} with time suggests increased solvent exposure of Trp 39 in the soluble oligomers.

When the same quenching conditions were applied to aliquots of the incubation *mixture* (i.e., insoluble and soluble material), the K_{sv} underwent an initial increase, as seen with the supernatant, followed by a major decrease, to a value of 1.8 M^{-1} after 108 h, demonstrating that the Trp is buried in the insoluble material (Figure 5B). Thus, the acrylamide quenching data also indicate that formation of fibrils leads to burial of Trp 39. The Stern−Volmer plots for the supernatant as a function of time are shown in Figure 5C. There were no significant changes in the static quenching component (K_{st}) as a function of incubation time.

(C) Fluorescence Anisotropy Changes during Aggregation. The fluorescence anisotropy of the *supernatant* of the incubation mixture was measured on the same samples that were used for intrinsic fluorescence and quenching measurements. Over the course of the first 40 h, the anisotropy showed a first-order decrease (Figure 6A). The decrease in anisotropy is rather surprising, since it could suggest a decrease in size of the aggregation species with increasing time. However, the most likely explanation is that the anisotropy reflects the local Trp mobility, and thus reflects increased mobility of Trp 39 with time, as the soluble oligomer species accumulates. This result is supported by the acrylamide quenching experiments which also showed a gradual increase in solvent accessibility of Trp with time. The anisotropy of the incubation *mixture* showed the anticipated increase (doubling over the period from 0 to 100 h) (Figure 6B), indicating either increased size of the fluorescent species and/or decreased mobility of Trp 39.

(D) Changes in ANS Binding during Aggregation. 1-Anilinonaphthalene-8-sulfonic acid (ANS) displays enhanced fluorescence and a characteristic blue shift in its fluorescence emission maximum from ∼515 to ∼475 nm when bound to protein hydrophobic surfaces and is especially useful in detecting partially folded conformations. The λ_{max} of ANS

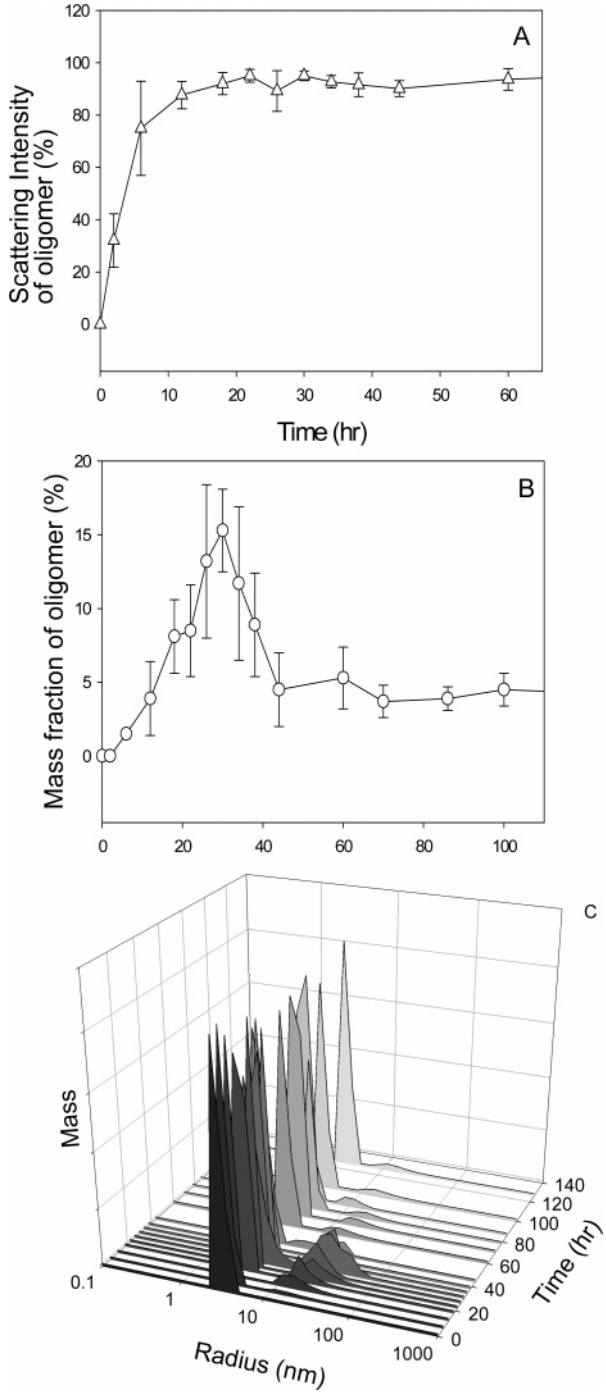

FIGURE 8: Dynamic light scattering analysis of Y39W incubation of supernatants reveals oligomeric intermediates. (A) Buildup of oligomers begins during the early stages of the lag phase, monitored by scattering intensity. (B) Scattering data presented as a fraction of the total protein mass present as oligomers during the incubation of Y39W. (C) Scattering traces, as mass fraction, during the incubation of Y39W. The smaller radius peaks correspond to monomeric Y39W.

binding to aliquots from the incubation *mixture* of Y39W, sampled at various time points, followed a sigmoidal profile, a mirror image of the ThT fluorescence curve. The signal remained constant at ~475 nm for the first 40 h, corresponding to the lag time and consistent with rapid initial formation of a partially folded conformation (probably initially monomeric and subsequently the oligomeric intermediate; see below) that binds ANS (Figure 7). The emission λ_{max} undergoes a significant blue shift once the lag time is over

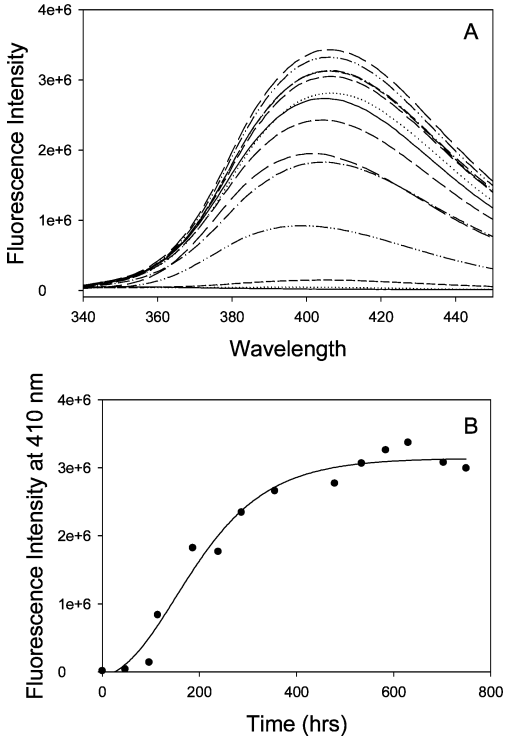

FIGURE 9: Formation of dityrosine in the soluble fraction during the incubation of Y39W α-synuclein, monitored by dityrosine fluorescence. (A) Dityrosine emission spectra as a function of time of incubation (see data point times in panel B) with excitation at 310 nm. The intensity at the λ_{max}, 410 nm, is plotted against time of incubation in (B). Fibril formation is complete before significant dityrosine fluorescence is detected. No dityrosine was detected in the insoluble fibrils.

and fibrils start to form (Figure 7). This demonstrates that ANS also binds to the fibrils and suggests an increased hydrophobic environment for ANS when bound to the fibrils and hence a very different conformation in the fibrils compared to the early oligomers. When the soluble material from aliquots was separated by centrifugation, the initial emission λ_{max} of 475 nm decreased to 465 nm by 12 h and remained there for the remainder of the incubation; parallel changes in intensity were also observed, with a 25% decrease in intensity from the monomer to the oligomeric intermediate(s).

(E) Oligomer Formation Monitored by Dynamic Light Scattering. To confirm the oligomeric state of Y39W α-synuclein during incubation at 37 °C, pH 7.4, we monitored aliquots of supernatant with dynamic light scattering (Figure 8). The initial aliquot showed only monomer, with $R_s = 3.1 \pm 0.2$ nm; however, by 3 h oligomeric species with $R_s = 22 \pm 2$ nm were observed (Figure 8C); with increasing time of incubation both the size and the size distribution (i.e., the polydispersity) of these oligomers increased somewhat. As shown in Figure 8B the concentration of these oligomers reached a maximum around 18 h (15% by mass of total protein) and then decreased. The lag time, measured by ThT in this experiment, was 25 h, due to slightly different incubation conditions. After completion of fibrillation as monitored by ThT, smaller oligomeric species were still present in the supernatant, with $R_s = 12-15$ nm. Figure 8A shows the mass fraction of oligomer and monomer during the lag time period and indicates that the oligomers are only a small fraction of the total soluble protein.

Scheme 1

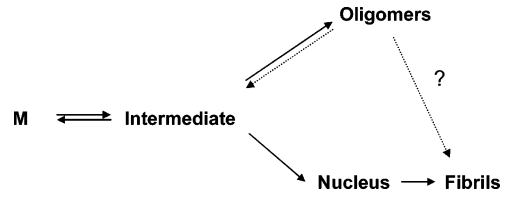

(F) Formation of Dityrosine. In preliminary experiments examining the intrinsic Trp fluorescence of the supernatant at long time periods we noted evidence for the formation of dityrosine. To ascertain if dityrosine was indeed being formed, we monitored dityrosine fluorescence for both supernatant and pellet as a function of incubation time. The data show that significant dityrosine formation occurs at long time periods, after fibrillation is complete (Figure 9). There was negligible fluorescence from dityrosine at 50 h, the end of the lag period, and very little signal at 100 h, after completion of fibril formation. However, significant dityrosine was evident by 120 h. Dityrosine arises from oxidation and is produced by covalent bond formation between two Tyr side chains involving tyrosyl radicals. No dityrosine fluorescence emission was observed in the fibrils at any times. Thus, the dityrosine must arise from the soluble material present after completion of fibrillation. It is interesting that the kinetics of dityrosine formation are sigmoidal (Figure 9B); the origin of such complex kinetics are not apparent at this time, except that detectable concentration of the late oligomer does not occur until after the lag period is over.

DISCUSSION

Incorporation of Trp into α-synuclein permits the use of a variety of new techniques, including solvent accessibility probes such as intrinsic fluorescence emission and acrylamide quenching, the presence of oligomers and the kinetics of their formation via fluorescence anisotropy, and changes in compactness via FRET. The use of a variety of complementary spectroscopic techniques allowed us to obtain information about the transient intermediate species during the fibrillation of Y39W α-synuclein. Interestingly, substitution of Tyr 39 by a Trp leads to a decrease in fibrillation rate, as well as a small increase in *β*-structure in the intrinsically disordered monomer, compared to wild-type α-synuclein.

There have been several recent reports regarding the conformation of monomeric α-synuclein. NMR studies show that monomeric α-synuclein is unfolded in solution but exhibits very rapid structural fluctuations including regions with a preference for helical conformation (*24*, *25*). The transient structures are stabilized by long-range interactions that fluctuate on the time scale of secondary structure formation during folding. Residue 39 in the monomer is in a region that becomes helical on binding to lipids and *β*-sheet in fibrils (*26*, *27*).

In the present study, several probes indicate the existence of a transient oligomeric intermediate(s) formed during the lag phase, prior to significant fibril formation (*28*). Scheme 1 shows our interpretation of the data in terms of a kinetic pathway for α-synuclein aggregation. The monomer (M) initially forms a partially folded intermediate (*23*, *29*) that partitions between the nucleated polymerization pathway leading to fibrils and off-pathway oligomeric intermediates (the early oligomers). The data do not allow us to distinguish whether these oligomers transform directly into fibrillar material or dissociate to monomers that then add to the growing fibrils. Even after fibrillation is complete, as indicated by no further increase in ThT signal, there is still some soluble α-synuclein present (∼15%). This material is at least partly oligomeric, based on SEC HPLC data, and could correspond to α-synuclein molecules that became oxidized, either at Met or at Tyr, or, alternatively, to stable associated states of the partially folded intermediate that became "entangled" and are unable to dissociate and go on to form fibrils.

Both the emission λ_{max} and the acrylamide quenching data for the monomer and the early oligomers indicate that Trp 39 is in a polar environment and probably fully exposed to the solvent. Time-resolved FRET has recently been used to monitor the conformation of monomeric α-synuclein using a set of donor Trp and nitrated Tyr acceptor pairs (*19*). One of these pairs involved a Trp at position 39 and a nitrated Tyr at position 19. The properties of the Trp in this variant were consistent with a highly mobile, solvent-exposed residue, as confirmed in the present study.

The Trp 39 is in the middle of the third repeat of α-synuclein. Its solvent exposure in the early oligomer indicates that this region of the protein is not only on the surface of the initially formed amyloidogenic partially folded intermediate but also in the subsequent associated state in the oligomers. The acrylamide quenching data for the supernatant show a gradual increase in the Stern−Volmer slope, K_{sv} during the lag phase, pointing to an increase in the exposure of the Trp with time. Presumably, this reflects changes in the local Trp 39 environment in the early oligomeric intermediate. Previous studies have shown that although the monomer of α-synuclein is significantly unfolded, it does possess limited structure and compactness (*30*−*34*), and the FTIR data reported here for monomeric Y39W α-synuclein suggest increased structure in the Trp variant; thus, a change in Trp mobility could reflect a change in the local structure about the Trp.

The decrease in fluorescence anisotropy implies either an increased rotational correlation time due to a decrease in molecular size or an increase in fluorophore mobility. The two most likely possibilities are an increase in the mobility of Trp 39 in the oligomeric intermediate or decreased size due to formation of the compact partially folded monomeric intermediate.

The Trp fluorescence emission of the fibrils has a blue-shifted λ_{max} compared to the monomer, indicating that Trp 39 is in a more nonpolar environment; however, the λ_{max} value of 346 nm suggests that the Trp environment is still in a somewhat polar environment. This could mean that Trp 39 is on the surface of the fibrils or that it is buried but surrounded by a significantly polar environment.

In summary, replacement of Tyr 39 by Trp in α-synuclein leads to slightly slower nucleation and slower fibril elongation, probably reflecting the changed hydrophobicity of the protein. The fact that changing one Tyr residue to one Trp leads to a 2-fold change in fibrillation rate indicates that very small changes in the physical properties of α-synuclein can have major effects on the kinetics of fibril formation, which, in turn, suggests a very finely balanced system. Characterization of monomeric Y39W shows that it is somewhat more

structured than the WT monomer, e.g., increased β-structure by FTIR. The fluorescence properties of the Trp variant demonstrate that Trp 39 is at least partially buried in the fibrils but solvent-exposed in the soluble species during α-synuclein aggregation and has increased local mobility during the lag phase compared to the monomer. ANS binding data also suggest a partially folded conformation throughout the lag phase. The dynamic light scattering results show the transient buildup of an oligomer during the lag phase, which subsequently decays. A smaller sized oligomer is observed during and after fibril formation. Maximum concentrations for both oligomers were around 15% of total protein. As the WT and Y39W proteins were shown to have very similar structures and fibrillation behavior, the results with Y39W α-synuclein can be extended to the WT as well.

REFERENCES

1. Lim, K. L., Dawson, V. L., and Dawson, T. M. (2003) The cast of molecular characters in Parkinson's disease: felons, conspirators, and suspects, *Ann. N.Y. Acad. Sci. 991*, 80−92.
2. Siderowf, A., and Stern, M. (2003) Update on Parkinson disease, *Ann. Intern. Med. 138*, 651−658.
3. Warner, T. T., and Schapira, A. H. (2003) Genetic and environmental factors in the cause of Parkinson's disease, *Ann. Neurol. 53* (Suppl. 3), S16−S23.
4. Kruger, R., Kuhn, W., Muller, T., Woitalla, D., Graeber, M., Kosel, S., Przuntek, H., Epplen, J. T., Schols, L., and Riess, O. (1998) Ala30Pro mutation in the gene encoding alpha-synuclein in Parkinson's disease, *Nat. Genet. 18*, 106−108.
5. Polymeropoulos, M. H., Lavedan, C., Leroy, E., Ide, S. E., Dehejia, A., Dutra, A., Pike, B., Root, H., Rubenstein, J., Boyer, R., Stenroos, E. S., Chandrasekharappa, S., Athanassiadou, A., Papapetropoulos, T., Johnson, W. G., Lazzarini, A. M., Duvoisin, R. C., Di Iorio, G., Golbe, L. I., and Nussbaum, R. L. (1997) Mutation in the alpha-synuclein gene identified in families with Parkinson's disease, *Science 276*, 2045−2047.
6. Spillantini, M. G., Crowther, R. A., Jakes, R., Hasegawa, M., and Goedert, M. (1998) alpha-Synuclein in filamentous inclusions of Lewy bodies from Parkinson's disease and dementia with lewy bodies, *Proc. Natl. Acad. Sci. U.S.A. 95*, 6469−6473.
7. Bradbury, J. (2003) Alpha-synuclein gene triplication discovered in Parkinson's disease, *Lancet Neurol. 2*, 715.
8. Miller, D. W., Hague, S. M., Clarimon, J., Baptista, M., Gwinn-Hardy, K., Cookson, M. R., and Singleton, A. B. (2004) Alpha-synuclein in blood and brain from familial Parkinson disease with SNCA locus triplication, *Neurology 62*, 1835−1838.
9. Singleton, A. B., Farrer, M., Johnson, J., Singleton, A., Hague, S., Kachergus, J., Hulihan, M., Peuralinna, T., Dutra, A., Nussbaum, R., Lincoln, S., Crawley, A., Hanson, M., Maraganore, D., Adler, C., Cookson, M. R., Muenter, M., Baptista, M., Miller, D., Blancato, J., Hardy, J., and Gwinn-Hardy, K. (2003) alpha-Synuclein locus triplication causes Parkinson's disease, *Science 302*, 841.
10. Betarbet, R., Sherer, T. B., and Greenamyre, J. T. (2002) Animal models of Parkinson's disease, *BioEssays 24*, 308−318.
11. Manning-Bog, A. B., McCormack, A. L., Li, J., Uversky, V. N., Fink, A. L., and Di Monte, D. A. (2002) The herbicide paraquat causes up-regulation and aggregation of alpha-synuclein in mice: paraquat and alpha-synuclein, *J. Biol. Chem. 277*, 1641−1644.
12. McCormack, A. L., and Di Monte, D. A. (2003) Effects of L-dopa and other amino acids against paraquat-induced nigrostriatal degeneration, *J. Neurochem. 85*, 82−86.
13. McCormack, A. L., Thiruchelvam, M., Manning-Bog, A. B., Thiffault, C., Langston, J. W., Cory-Slechta, D. A., and Di Monte, D. A. (2002) Environmental risk factors and Parkinson's disease: selective degeneration of nigral dopaminergic neurons caused by the herbicide paraquat, *Neurobiol. Dis. 10*, 119−127.
14. Thiruchelvam, M., McCormack, A., Richfield, E. K., Baggs, R. B., Tank, A. W., Di Monte, D. A., and Cory-Slechta, D. A. (2003) Age-related irreversible progressive nigrostriatal dopaminergic neurotoxicity in the paraquat and maneb model of the Parkinson's disease phenotype, *Eur. J. Neurosci. 18*, 589−600.
15. Zarranz, J. J., Alegre, J., Gomez-Esteban, J. C., Lezcano, E., Ros, R., Ampuero, I., Vidal, L., Hoenicka, J., Rodriguez, O., Atares, B., Llorens, V., Gomez, T. E., del Ser, T., Munoz, D. G., and de Yebenes, J. G. (2004) The new mutation, E46K, of alpha-synuclein causes Parkinson and Lewy body dementia, *Ann. Neurol. 55*, 164−173.
16. Weinreb, P. H., Zhen, W., Poon, A. W., Conway, K. A., and Lansbury, P. T., Jr. (1996) NACP, a protein implicated in Alzheimer's disease and learning, is natively unfolded, *Biochemistry 35*, 13709−13715.
17. Lavedan, C., Leroy, E., Dehejia, A., Buchholtz, S., Dutra, A., Nussbaum, R. L., and Polymeropoulos, M. H. (1998) Identification, localization and characterization of the human gamma-synuclein gene, *Hum. Genet. 103*, 106−112.
18. Lavedan, C., Leroy, E., Torres, R., Dehejia, A., Dutra, A., Buchholtz, S., Nussbaum, R. L., and Polymeropoulos, M. H. (1998) Genomic organization and expression of the human beta-synuclein gene (SNCB), *Genomics 54*, 173−175.
19. Lee, J. C., Langen, R., Hummel, P. A., Gray, H. B., and Winkler, J. R. (2004) {alpha}-Synuclein structures from fluorescence energy-transfer kinetics: Implications for the role of the protein in Parkinson's disease, *Proc. Natl. Acad. Sci. U.S.A. 101*, 16466−16471.
20. Nielsen, L., Khurana, R., Coats, A., Frokjaer, S., Brange, J., Vyas, S., Uversky, V. N., and Fink, A. L. (2001) Effect of environmental factors on the kinetics of insulin fibril formation: elucidation of the molecular mechanism, *Biochemistry 40*, 6036−6046.
21. Eftink, M. R., and Ghiron, C. A. (1981) On the analysis of the temperature and viscosity dependence of fluorescence-quenching reactions with proteins, *Arch. Biochem. Biophys. 209*, 706−709.
22. Oberg, K. A., and Fink, A. L. (1995) Methods for collecting and analyzing attenuated total reflectance FTIR spectra of proteins in solution, in *Techniques in Protein Chemistry* (Crabb, W., Ed.) pp 475−484, Academic Press, New York.
23. Uversky, V. N., Li, J., and Fink, A. L. (2001) Evidence for a partially folded intermediate in alpha-synuclein fibril formation, *J. Biol. Chem. 276*, 10737−10744.
24. Eliezer, D., Kutluay, E., Bussell, R., Jr., and Browne, G. (2001) Conformational properties of alpha-synuclein in its free and lipid-associated states, *J. Mol. Biol. 307*, 1061−1073.
25. Bertoncini, C. W., Jung, Y. S., Fernandez, C. O., Hoyer, W., Griesinger, C., Jovin, T. M., and Zweckstetter, M. (2005) Release of long-range tertiary interactions potentiates aggregation of natively unstructured alpha-synuclein, *Proc. Natl. Acad. Sci. U.S.A. 102*, 1430−1435.
26. Jao, C. C., Der-Sarkissian, A., Chen, J., and Langen, R. (2004) Structure of membrane-bound {alpha}-synuclein studied by site-directed spin labeling, *Proc. Natl. Acad. Sci. U.S.A. 101*, 8331−8335.
27. Der-Sarkissian, A., Jao, C. C., Chen, J., and Langen, R. (2003) Structural organization of alpha-synuclein fibrils studied by site-directed spin labeling, *J. Biol. Chem. 278*, 37530−37535.
28. Bitan, G., Ding, T. T., Kirkitadze, M. D., Lansbury, P. T., Teplow, D. B., Lomakin, A. V., and Benedek, G. B. (2002) Biophysical studies of the initial oligomerization events in amyloid-protein assembly, *Neurobiol. Aging 23*, S556.
29. Uversky, V. N., and Fink, A. L. (2004) Conformational constraints for amyloid fibrillation: the importance of being unfolded, *Biochim. Biophys. Acta 1698*, 131−153.
30. Munishkina, L. A., Phelan, C., Uversky, V. N., and Fink, A. L. (2003) Conformational behavior and aggregation of alpha-synuclein in organic solvents: Modeling the effects of membranes, *Biochemistry 42*, 2720−2730.
31. Uversky, V. N., Li, J., Souillac, P. O., Millett, I. S., Doniach, S., Jakes, R., Goedert, M., and Fink, A. L. (2002) Biophysical properties of the synucleins and their propensities to fibrillate: inhibition of alpha-synuclein assembly by beta- and gamma-synucleins, *J. Biol. Chem. 277*, 11970−11978.
32. Uversky, V. N., Yamin, G., Souillac, P. O., Goers, J., Glaser, C. B., and Fink, A. L. (2002) Methionine oxidation inhibits fibrillation of human alpha-synuclein in vitro, *FEBS Lett. 517*, 239−244.
33. Uversky, V. N., and Fink, A. L. (2002) Biophysical properties of human alpha-synuclein and its role in Parkinson's disease, *Recent Res. Dev. Protein Eng. 1*, 186.
34. Li, J., Uversky, V. N., and Fink, A. L. (2001) Effect of familial Parkinson's disease point mutations A30P and A53T on the structural properties, aggregation, and fibrillation of human alpha-synuclein, *Biochemistry 40*, 11604−11613.

BI051426Z